View Article Online / Journal Homepage / Table of Contents for this issue

From vesicles to solid spheres: terminal functional group induced morphology modification†

Qi Wang, Junchen Wu, Zuguang Gong, Ying Zou, Tao Yi* and Chunhui Huang

Received 5th January 2010, Accepted 22nd March 2010
First published as an Advance Article on the web 5th May 2010
DOI: 10.1039/b927579g

Published on 05 May 2010. Downloaded by University at Buffalo Libraries on 14/10/2014 15:32:00.

Two similar naphthalimide based organogelators were synthesized. These two compounds can gelate a variety of organic solvents and form interesting morphologies. Transmission and scanning electron microscopy of the xerogels of the two compounds showed vesicle and solid sphere morphologies, respectively, even though their molecular structures are very close. The mechanism of the self-assembly process was investigated by ^{1}H NMR, IR, 2D-NOESY spectra, wide-angle X-ray diffraction and rheological experiments. The study reveals that the cooperation and competition of multiple intra/inter-molecular interactions are the main determining factors for these compounds' self-assembly into vesicles and solid spheres. A single functional group able to determine the formation of vesicles in non-typical amphiphilic system is rarely encountered. Therefore, these results provide further insights into morphology control, especially the formation of vesicles in non-typical amphiphilic systems.

Introduction

Vesicles have been extensively studied over the past decades for their potential applications in drug delivery,[1] templates for processing well-defined materials and food processing.[2] As we already know, numerous amphiphilic polymers, surfactants and lipids can form vesicles through self-organization.[3] Recently, vesicles formed from low weight molecules through noncovalent interactions have also been attracting attention.[4] For example, Shinkai and co-workers reported a diazacrown-appended cholesterol gelator that could assemble into vesicles and then, by vesicle-vesicle interactions, yield an extended network.[4a] Li and co-workers presented the first example of a non-typical amphiphilic structure containing no hydrophilic segment which could form vesicles in polar methanol and assemble into fibrillar gels in apolar solvents.[4b] Taking into account the dynamic character of those vesicles, they may show advantages in biomedical applications and smart materials. Despite a wide range of reported smart materials capable of self-organizing with high efficiency and selectivity,[5] the design of nonamphiphilic structures which can be controlled by changing the building blocks that spontaneously form vesicles and balls has rarely been reported.

Considering the large amount of complicated noncovalent intermolecular interactions such as H bonds, π–π interactions, steric hindrance as well as hydrophobic/hydrophilic interactions during the assembly of the molecules, it is really a challenge to achieve controllable self-assembly through modulation of the molecular structure. Our group previously reported a class of naphthalimide derivative gels which formed various morphologies in response to outside stimuli, such as sonication and chemical input.[6] In this work, we attached pyridine as a terminal group to compound **1a** (Scheme 1a). This terminal pyridine group may act as a proton acceptor to form hydrogen bonds with the proton of amide in the linker, thus tuning the structure for self-assembly. For comparison, compound **1b** with a terminal methylphenyl group replacing pyridine was also synthesized. It is surprising that the self-assembly of the two compounds showed quite different vesicle and solid sphere morphologies, respectively, in spite of their molecular structures being very similar. This may be the first example of a non-typical amphiphilic naphthalimide derivative whose morphology can be controllably altered from vesicles to solid spheres by modulation of the building blocks.

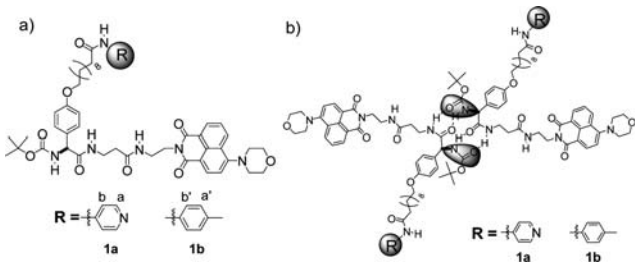

Scheme 1 a) Molecular structures of **1a** and **1b**; b) proposed antiparallel β-sheet model for compounds **1a** and **1b** in the gel.

Experimental

General methods

All starting materials were obtained from commercial suppliers and used as received. ^{1}H NMR and ^{13}C NMR spectra were recorded on a Mercuryplus, at 400 and 100 MHz, respectively. Proton chemical shifts are reported in parts per million downfield from tetramethylsilane. 2D spectra were recorded using a Bruker DRX-500 spectrometer. Standard Bruker pulse sequences were

Department of Chemistry & Laboratory of Advanced Materials, Fudan University, Shanghai, 200433, P. R. China. E-mail: yitao@fudan.edu.cn; Fax: +86-21-55664621; Tel: +86-21-55664185

† Electronic supplementary information (ESI) available: Details of synthesis and spectroscopic characterisation of the compounds. See DOI: 10.1039/b927579g

View Article Online

Published on 05 May 2010. Downloaded by University at Buffalo Libraries on 14/10/2014 15:32:00.

used for the experiments. Matrix assisted laser desorption ionization time-of-flight (MALDI-TOF) mass spectra were recorded on an AXIMA-CFRPLVS mass spectrometer (Shimadzu). ESI-MS data were recorded on a Waters Quattro Micro API LC-MS-MS spectrometer (Waters, USA). Element analysis was carried out on a VARIOEL3 apparatus (ELEMENTAR). Melting points were determined on a hot-plate melting point apparatus XT4-100A. All solutions were absolute anhydrous.

Wide-angle X-ray scattering

Experiments were performed on a SAXSess high-flux small-angle X-ray scattering instrument (Anton Paar) equipped with a Kratky block-collimation system at room temperature. The X-rays were generated by using a Philips PW3830 sealed-tube X-ray generator (Cu target, $\lambda = 0.1542$ nm) with a power of 40 kV and 50 mA. Gels of **1a** and **1b** were measured in glass capillaries. The incident X-ray beam was perpendicular to the long axis of the capillary. The diffraction data were corrected for background scattering.

Rheology

Experiments were performed on a MCR 301 Anton Paar (Austria) rheometer, with a Couette cell and a temperature control unit. The measurements were carried out on freshly prepared gels by using a controlled-stress rheometer. Parallel-plate geometry of 25 mm diameter and 1 mm gap were employed throughout the dynamic oscillatory tests. The following tests were performed: increasing amplitude of oscillation up to 100% apparent strain shear (kept a frequency of 1 rad s^{-1}) and frequency sweeps at 20 °C (from 100–0.1 rad s^{-1}, 0.1% strain).

Transmission and scanning electron microscopy

A JEOL JEM-2100 F (UHR) mode field-emission transmission electron microscope was used for TEM imaging, operating at 200 kV and fitted with an EDX analysis accessory. The samples were prepared by coating the diluted wet gels onto a copper grid covered with Formvar film at room temperature and the samples were then transferred into a freeze drier (EYELA, FDU-1200) for 24 h. A Shimadzu SUPERSCAN SSX-550-SEM was used for SEM imaging with an accelerating voltage of 15 kV. The wet gel samples were firstly diluted and applied to the moulds (40 mm × 40 mm square shaped, 0.5 mm thick mica plates) in four different concentrations. Thereafter, the samples in the moulds were transferred into a freeze drier (EYELA, FDU-1200) for 24 h and coated with Au.

Fluorescent and IR spectra

The fluorescent spectra were recorded with a LFS920 (Edinburgh) spectrophotometer equipped with a 1000 W xenon lamp as the excitation source. Fourier transform infrared (FTIR) spectra were measured using an IRPRESTIGE-21 spectrometer (Shimadzu) with KBr pellets.

Gelation test for organic fluids

The gelators and solvents were put in a septum-capped test tube and heated (>75 °C) until the solid was dissolved. The sample vial was then cooled to 25 °C (room temperature). Qualitatively, gelation was considered successful if no sample flow was observed upon inversion of the container at room temperature (the inverse flow method).

Results and discussion

Synthesis and characterization

Two naphthalimide derivatives **1a** and **1b** containing dipeptides with different functional building blocks **R** (**1a**, pyridine; **1b**, methylphenyl) were designed for the purpose of studying the morphology control of the molecules in the self-organizing process. Details of synthesis and characterization of **1a** and **1b** are described in the electronic supplementary information (ESI).† The first step of synthesis was the preparation of two different terminal groups connected by a long alkyl chain (Scheme 2). Treatment of 11-bromoundecanoic acid in thionyl chloride generated an acyl chloride compound which was reacted with 4-amino-pyridine and *p*-methylaniline to afford two single peptide compounds **2a** and **2b**, respectively.

The protection of L-tyrosine was begun by reacting it with thionyl chloride in methanol for 3 h. The functional amino group of compound **3** was further protected by reacting it with Boc_2O in the presence of triethylamine in distilled THF. Compounds **6a** and **6b** were synthesized by the reaction of compounds **2a** and **2b** with the corresponding phenolic hydroxyl group of compound **4** followed by regenerating the active carboxylic acid group of the L-tyrosine moiety in lithium hydroxide solution.

Compounds **1a** and **1b** were synthesized by the reaction of the naphthalic precursor as previously synthesized by our group with **6a** and **6b** in the presence of dicyclohexylcarbodiimide in dichloromethane solution. Structural characterization of all the compounds was carried out by ^{1}H, ^{13}C NMR and mass spectroscopy.

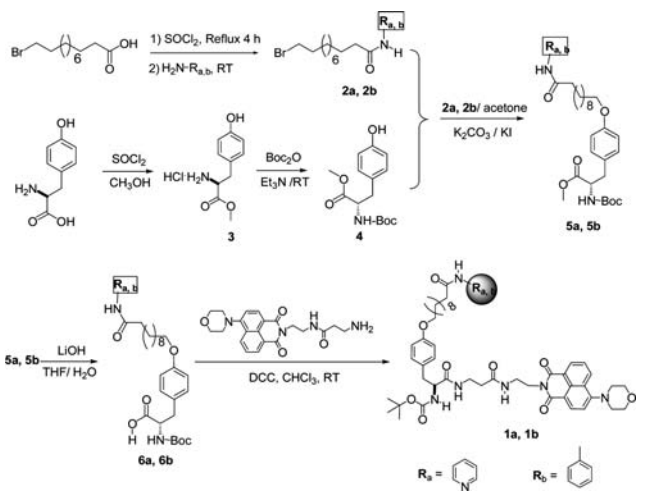

Scheme 2 Synthesis route to compounds **1a** and **1b**.

 This journal is © The Royal Society of Chemistry 2010

View Article Online

Published on 05 May 2010. Downloaded by University at Buffalo Libraries on 14/10/2014 15:32:00.

Gelation properties of the compounds

The organogels were obtained after the hot solution of **1a** or **1b** had been cooled to room temperature (25 °C) and aged for at least 30 min. As expected, **1a** and **1b** can specifically gelate certain organic solvents.[7] However, the specific gelation abilities of **1a** and **1b** are completely different even though they have similar structures (Table 1). **1a** could form transparent gels in alcohols (ethanol, isopropanol, *n*-propanol) and 1,4-dioxane. In contrast, **1b** was barely soluble in most alcohols, even methanol, but can form gels in acetonitrile. The critical gelation concentration (CGC) of **1b** is rather low (5 mg mL^{-1}) compared with **1a** (25 mg mL^{-1}). Upon heating (>80 °C), all gels of **1a** and **1b** could easily be converted into the original sol and retransformed to gels by cooling the sol to room temperature and aging for about one hour. Comparison of the gelation ability of the two compounds implies that the two different terminal groups significantly influence gel formation. By changing the pyridine moiety (**1a**) to methylphenyl (**1b**), the gelation solvents and the CGC are dramatically changed. Furthermore; in polar solvents, **1a** more easily forms transparent gels while in non-polar solvents the gelation behavior of **1b** is stronger.

Morphology of the gels

To gain better insight into the molecular organization in gel form, the morphologies of xerogels obtained from **1a** and **1b** were investigated by scanning electron microscopy (SEM) (Fig. 1). In acetonitrile and low molecular weight alcohols, **1a** self-assembled into spherical vesicles of differing diameters from 100–500 nm (Fig. 1a–c). Vesicles formed in *i*-propanol were more uniform (Fig. 1c). In high molecular weight alcohols such as *n*-propanol a caky structure was observed (Fig. 1d). In 1-hexanol and S-(+)-2-octanol, the morphology of the xerogels revealed fibrous structure (Fig. 1e, f); while in 1,4-dioxane, burl-like superstructure of 2–3 μm size was observed (Fig. 1g). The sphere morphology was also observed in the SEM image of the **1b** xerogel from acetonitrile with a diameter of 50–120 nm (Fig. 1h). Interestingly, compared to **1a**, the diameter of the spheres is much smaller (60 nm on average). However, evaporated from solvents that do not form gels, the powder of **1a** from ethyl acetate and acetone shows a burl-like structure of 5 to 10 μm size, whereas **1b** shows needle structures in ethanol and acetone (ESI†).

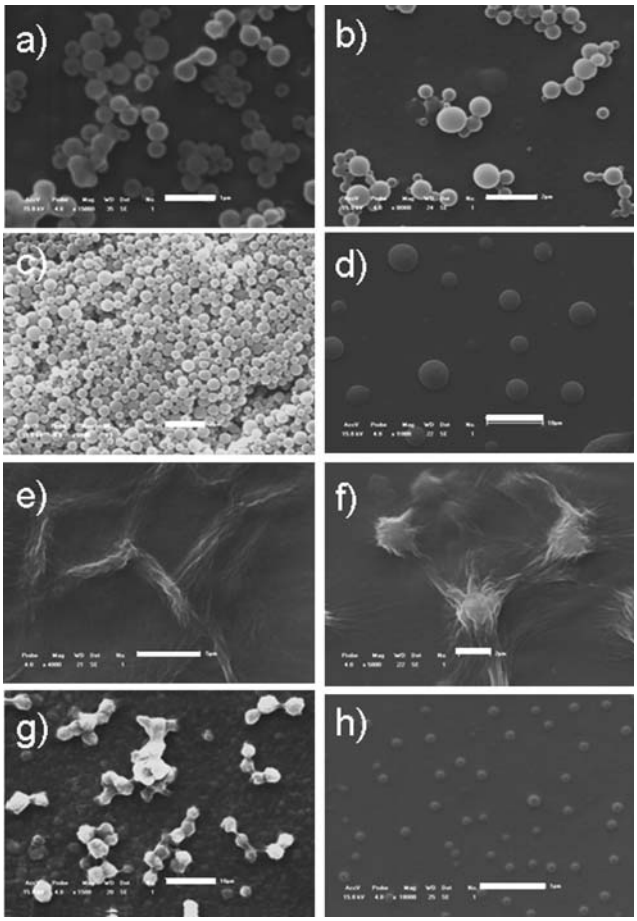

Fig. 1 SEM images of the xerogels at room temperature (25 °C). **1a** in a) acetonitrile, b) ethanol, c) isopropanol, d) *n*-propanol, e) 1-hexanol, f) S-(+)-2-octanol, g) 1,4-dioxane (20 mg mL^{-1}) and h) **1b** in acetonitrile (5 mg mL^{-1}). The concentrations of the gels are 25 mg mL^{-1} except where otherwise mentioned. Scale bar: a) 1 μm; b) 2 μm; c) 2 μm; d) 10 μm; e) 5 μm; f) 2 μm; g) 10 μm; h) 1 μm.

Table 1 Gelation ability of **1a** and **1b**[a]

Solvent	**1a**[b]	**1b**[b]
Methanol	S	I
Ethanol	G (30)	I
i-Propanol	G (25)	I
n-Propanol	G (25)	I
Dichloromenthane	S	S
Chloroform	S	S
Acetone	PG	P
Toluene	S	PG
Tetrahydrofuran	S	I
Acetonitrile	PG	G (5)
1,4-Dioxane	G (25)	I
Xylene	I	PG
Benzene	I	I

[a] G: gel; PG: partial gel; P: precipitation; S: solution; I: insoluble. The critical gelation concentrations of the gelators are given in parentheses (mg mL^{-1}). [b] Heated to dissolve and cooled to room temperature then aged for 30 min (25 °C).

TEM images also reveal important information about the superstructures. The hollowness of **1a** vesicles was confirmed by TEM images (Fig. 2a,b). TEM images clearly show the **1a** xerogel in acetonitrile forming hollow spheres with the diameter of about 200 nm. The wall thickness of the vesicles was estimated to be 20–25 nm (Fig. 2b). Similar results were also observed for **1a** in ethanol and *i*-propanol. Different from the hollow vesicle structure of **1a**, TEM images of the **1b** xerogel from acetonitrile indicate the formation of solid balls with a diameter of about 60–90 nm (Fig. 2c). Each ball is in turn composed of smaller domains with a diameter of less than 10 nm (Fig. 2d). It is evident that by changing the pyridine (**1a**) to the methylphenyl (**1b**) of the aliphatic chains the morphology changed from big vesicles to a certain kind of smaller solid spheres. The different structures reveal that the self-assembly process of the molecules strongly depends on the functional moiety of the appended alkyl chains, as well as on the gelation solvent.

View Article Online

Published on 05 May 2010. Downloaded by University at Buffalo Libraries on 14/10/2014 15:32:00.

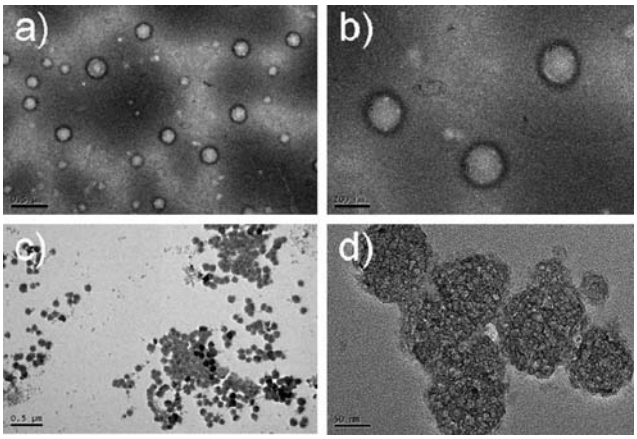

Fig. 2 TEM images of the xerogels: (a, b) **1a** in acetonitrile (25 mg mL^{-1}); (c, d) **1b** in acetonitrile (5 mg mL^{-1}). Scale bar: a) 0.5 μm; b) 200 nm; c) 0.5 μm; d) 50 nm.

Rheology

The mechanical properties of **1a** and **1b** gels were studied by dynamic oscillatory measurements (Fig. 3). The linear viscoelastic regions (LVR) of gels **1a** and **1b** were determined by strain amplitudes ranging from 0.01 to 100% at 6.28 rad s^{-1}. Both the storage modulus (G') and loss modulus (G'') remain constant up to approximately 0.5% strain ($G' > G''$). Interestingly, beyond this level of deformation, **1a** shows a weak strain overshoot[8] so that the G' of **1a** decreases, while the G'' increases to form a small peak and then decreases (Fig. 3a). Dynamic oscillatory data show that, when a small strain was imposed, the G' and G'' of the **1a** and **1b** gels remain constant (linear region). The small peak appearing at 0.5% strain in the **1a** gel may be attributed to the breakage of the spherical structure into layers, which causes an increase in the loss modulus (G'').[9] In sharp contrast to **1a**, such a kind of overshoot does not appear in the **1b** gel. The **1b** gel shows a catastrophic disruption which is indicated by a step decrease in the values of both moduli and the reversal of the viscoelastic signal ($G'' > G'$; Fig. 3a). This result indicates that **1b** forms an intercrossed morphology rather than the hollow spheres. The implementation of a frequency sweep between 0.1 and 100 rad s^{-1} shows $G' > G''$ which confirms that gels **1a** and **1b** have predominantly elastic character (Fig. 3b). Thus, these results further establish the difference of morphologies and self-assemblies between **1a** and **1b**.

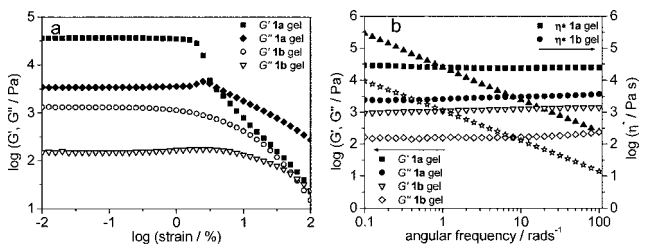

Fig. 3 Dynamic oscillatory data for **1a** and **1b** gel at 20 °C. a) Strain sweep of gels at a frequency of 6.28 rad s^{-1}. b) Frequency sweep of gels at a strain of 0.1%. Gels: **1a**, 25 mg mL^{-1} in *i*-propanol; **1b**, 10 mg mL^{-1} in acetonitrile.

Spectral study

To gather information at the molecular level, liquid state ^{1}H NMR experiments were performed. A 2D-NOESY spectrum of a d_6-DMSO solution of compound **1a** at 273 K revealed a unique conformation of the chiral carbon in the L-tyrosine moiety. NOE cross-peaks are in line with an *anti* conformation representing the two amide functions (connected to the L-tyrosine) in opposite directions (Fig. S2, ESI†).[10] Such a conformation is favorable for the organization of compound **1a** into β-sheet structures *via* intermolecular H-bonding (Scheme 1b). Temperature-dependent ^{1}H NMR shows that the signals for H_a and H_b in the pyridine unit of **1a** were shifted upfield by 0.03 and 0.02 ppm, respectively, from 30 to 70 °C (Fig. 4). The chemical shift of protons in pyridine with the change of temperature indicates that pyridine forms an intramolecular H-bond with the amide group. The increasing temperature weakens the intramolecular H-bond thus causing a chemical shift of protons in pyridine. In contrast, similar phenomena didn't appear in compound **1b**. The small peaks around 7.6 ppm correspond to the amide groups of **1a** and **1b** both shifted upfield by 0.25 ppm. Concentration-dependent ^{1}H spectra (6.5–39 mM) of **1a** show a chemical shift of about 0.03 ppm for the naphthalic group due to π–π stacking; while no chemical shift in the pyridine moiety was observed (Fig.S3, ESI†). The ^{1}H NMR spectra indicate that π–π interactions became stronger as the concentration increased. On the other hand, temperature can also strongly affect the intra- and inter-molecular H-bonding during the gelation process.

Fluorescent spectra show concentration-dependent emission in both **1a** and **1b** (Fig. S4, ESI†). Compounds **1a** and **1b** exhibit similar emission spectra in solution. In particular, the maximum emission wavelength of **1a** and **1b** shifted from 518 to 532 nm and 514 to 524 nm, respectively, when the concentration increased from 0.1 to 20 mM. This suggests that **1a** and **1b** have strong π–π interactions in the more concentrated state as compared with a more diluted one.

In order to check the contribution of hydrogen bonds in the amide and carbamate groups to the gelation process, the infrared

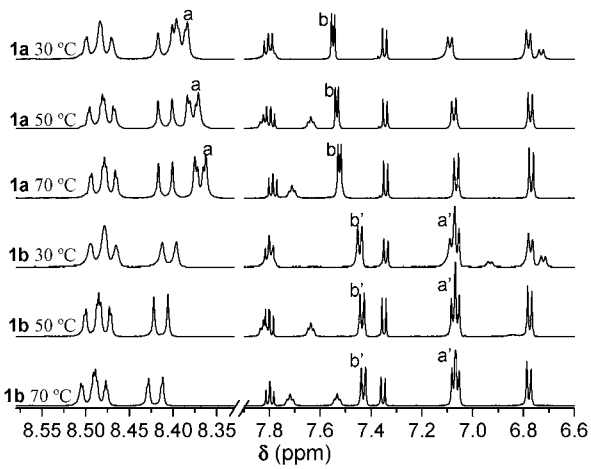

Fig. 4 ^{1}H NMR spectra (500 MHz) of **1a** (2 mM) and **1b** (2 mM) at 30, 50 and 70 °C in DMSO. The signals marked a and b correspond to the protons of **1a** and the signals marked a′ and b′ correspond to the protons of **1b** which are mentioned in Scheme 1.

 This journal is © The Royal Society of Chemistry 2010

View Article Online

Published on 05 May 2010. Downloaded by University at Buffalo Libraries on 14/10/2014 15:32:00.

spectra of **1a** and **1b** were measured in acetonitrile. The N–H stretching bands were examined. The IR spectra of gel samples of **1a** and **1b** showed a strong NH stretching band at 3312 cm^{-1} which indicates that strong intermolecular H-bonding exists in both **1a** and **1b** gels (Fig. S5, ESI†).[4b]

Wide-angle X-ray scattering

The molecular packing of **1a** and **1b** in the xerogel was further investigated by powder X-ray diffraction (Fig. 5). The scattering patterns of the **1a** xerogel in acetonitrile and *i*-propanol show a sharp peak in the range of 4.5–4.7 nm. Molecular modeling suggested that the self-assembly of the **1a** dimer had a spacing distance of approximately 4.5 nm. Considering the contribution of the intermolecular H-bonding, this result supports the view that the ordered structure was generated through intermolecular H-bonding and π–π stacking (Fig. 6). The **1b** xerogel of acetonitrile displays a completely different X-ray diffraction profile, with two peaks corresponding to *d* spacings of 5.6 and 0.97 nm. These two peaks correspond to the framework of self-assembly molecular layers and the average distance between the stacked foldamers, respectively. Interestingly, the aggregation of β-sheet monolayers of **1a** and **1b** in the xerogel phase was also clearly identified by their XRD patterns. All the xerogel samples feature a peak at about 0.46 nm, which is a typical value for the inter-strand distance of β sheets.[11]

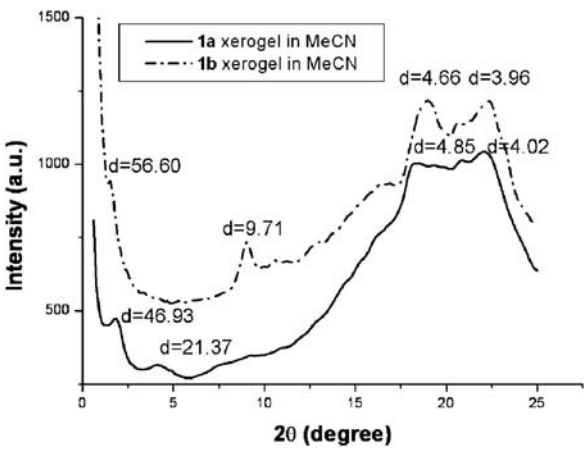

Fig. 5 X-Ray diffraction patterns of **1a** and **1b** xerogels in acetonitrile at room temperature (**1a**, solid line; **1b**, dash dot line).

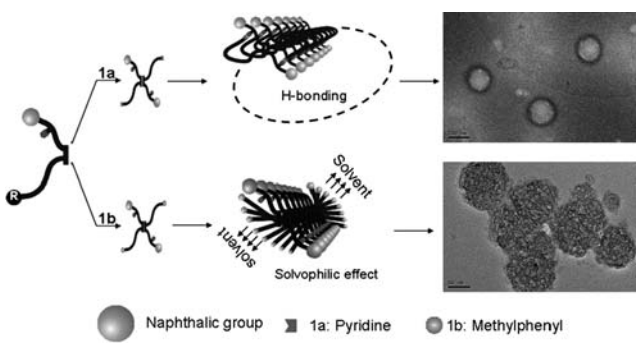

Fig. 6 Tentative model for the self-assembly of vesicles and balls from compounds **1a** and **1b**.

Relation between morphologies and gel mechanical properties

The present results reveal that it is a thermodynamic balance among the hydrogen bonding, π–π interaction and solvophilic effect which makes the molecules self-assemble into the different morphologies. Thus, we can propose that the vesicles of **1a** were composed of multi-layers of self-assembled molecules as indicated by the space-filling model and TEM image.[12] These layers were generated by two-dimensional packing of the dimers through π–π interactions of the naphthalic moieties. During the formation of the vesicles, the pyridine functional moiety with the appended alkyl chains entangled with each other by intramolecular hydrogen bonding, which interlocked the dimers and formed the vesicles (Fig. 6). In contrast, the formation of the solid balls of **1b** may mainly be due to the effect of the terminal methylphenyl group. During the gelation process, the appended flexible alkyl chains try to extend to the exterior of the assembly framework by solvophilic effects instead of being entangled with each other by H-bonding interactions. This would inhibit **1b** from self-assembling into a bigger network. As a result, compound **1b** can only form small solid balls. The small balls further aggregate into bigger balls by van der Waals interactions and π–π stacking. The result proves that the two different terminal groups are the key determinants for the formation of the two different morphologies from vesicles to solid balls. It should also be mentioned that the solvent may also play an important role in determining the formation of self-assembly structures.

Conclusions

In this work, we have successfully synthesized two naphthalimide based organogels which could self-assemble to form vesicles and spheres. Intermolecular hydrogen bonding, π–π stacking and van der Waals interactions stabilize the rigid conformations of compound **1a** to form vesicles. When the pyridine moiety of **1a** was changed to methylphenyl (**1b**), both the gelation properties and morphology were changed dramatically. The different morphologies formed by **1a** and **1b** illustrate that the self-assembly of the peptides can be easily changed by modulating the appended functional groups. These results provide a deeper understanding of the gel formation process of non-typical amphiphilic compounds. Moreover, it may open the way to studying the effect of appending moieties on the gel formation process. The well defined hydrophilic hollow vesicles could be used in various applications, such as biomimetic studies, drug and gene delivery systems and responsive materials. We intend to explore some of these possibilities in our future research.

Acknowledgements

This work was supported by the National Science Foundation of China (grant no. 20771027), the National Basic Research Program of China (grant no. 2009CB930400), Specialized Research Fund for the Doctoral Program of Higher Education (grant no. 200802460007), Shanghai Sci. Tech. Comm. (grant no. 08JC1402400), and the Shanghai Academic discipline project (no. B108).

View Article Online

Published on 05 May 2010. Downloaded by University at Buffalo Libraries on 14/10/2014 15:32:00.

References

1 (*a*) G. Haering and P. L. Luisi, *J. Phys. Chem.*, 1986, **90**, 5892–5895; (*b*) J. F. Miravet and B. Escuder, *Org. Lett.*, 2005, **7**, 4791–4794; (*c*) E. Soussan, S. Cassel, M. Blanzat and I. Rico-Lattes, *Angew. Chem., Int. Ed.*, 2009, **48**, 274–288; (*d*) D. Paolino, D. Cosco, M. Licciardi, G. Giammona, M. Fresta and G. Cavallaro, *Biomacromolecules*, 2008, **9**, 1117–1130; (*e*) E. P. Holowka, V. Z. Sun, D. T. Kamei and T. J. Deming, *Nat. Mater.*, 2007, **6**, 52–57; (*f*) X. Guo and F. C. SzokaJr, *Acc. Chem. Res.*, 2003, **36**, 335–341.

2 (*a*) D. E. Discher and A. Eisenberg, *Science*, 2002, **297**, 967–973; (*b*) S. J. Rowan, S. J. Cantrill, G. R. L. Cousins, J. K. M. Sanders and J. F. Stoddart, *Angew. Chem., Int. Ed.*, 2002, **41**, 898–952; (*c*) R. Blumenthal, M. J. Clague, S. R. Durell and R. M. Epand, *Chem. Rev.*, 2003, **103**, 53–70; (*d*) H. Li, J. Liu, S. Xie, M. Qiao, W. Dai, Y. Lu and H. Li, *Adv. Funct. Mater.*, 2008, **18**, 3235–3241; (*e*) H. Wang, Y. Wang, X. Zhou, L. Zhou, J. Tang, J. Lei and C.-Z. Yu, *Adv. Funct. Mater.*, 2007, **17**, 613–617; (*f*) L. Zhang, P. Li, X. Liu, L. Du and E. Wang, *Adv. Mater.*, 2007, **19**, 4279–4283; (*g*) D. H. W. Hubert, M. Jung and A. L. German, *Adv. Mater.*, 2000, **12**, 1291–1294.

3 (*a*) M. A. Hillmyer, *Science*, 2007, **317**, 604–605; (*b*) I. W. Hamley and V. Castelletto, *Angew. Chem., Int. Ed.*, 2007, **46**, 4442–4455; (*c*) T. M. Allen and P. R. Cullis, *Science*, 2004, **303**, 1818–1822; (*d*) Y. Wang, H. Xu and X. Zhang, *Adv. Mater.*, 2009, **21**, 2849–2864; (*e*) J.-M. Lehn, *Science*, 2002, **295**, 2400–2403; (*f*) I. W. Hamley, *Soft Matter*, 2005, **1**, 36–43; (*g*) M.-H. Li and P. Keller, *Soft Matter*, 2009, **5**, 927–937.

4 (*a*) J. H. Jung, Y. Ono, K. Sakurai, M. Sano and S. Shinkai, *J. Am. Chem. Soc.*, 2000, **122**, 8648–8653; (*b*) W. Cai, G.-T. Wang, Y. Xu, X.-K. Jiang and Z.-T. Li, *J. Am. Chem. Soc.*, 2008, **130**, 6936–6937; (*c*) A. Ajayaghosh and V. K. Praveen, *Acc. Chem. Res.*, 2007, **40**, 644–656; (*d*) A. Ajayaghosh, R. Varghese, V. K. Praveen and S. Mahesh, *Angew. Chem., Int. Ed.*, 2006, **45**, 3261–3264; (*e*) H. Lee, K. Park, Y. Jeon, D. Kim, D. Oh, H. Kim, C. Park and K. Kim, *J. Am. Chem. Soc.*, 2005, **127**, 5006–5007.

5 (*a*) W. Cai, G.-T. Wang, P. Du, R.-X. Wang, X.-K. Jiang and Z.-T. Li, *J. Am. Chem. Soc.*, 2008, **130**, 13450–13459; (*b*) Z.-T. Li, J.-L. Hou and C. Li, *Acc. Chem. Res.*, 2008, **41**, 1343–1353; (*c*) S. Zhou, C. Burger, B. Chu, M. Sawamura, N. Nagahama, M. Toganoh, U. E. Hackler, H. Isobe and E. Nakamura, *Science*, 2001, **291**, 1944–1947; (*d*) J. Zhou, X. Chen and Y. Zheng, *Chem. Commun.*, 2007, (48), 5200–5202.

6 (*a*) J. Wu, T. Yi, T. Shu, M. Yu, Z. Zhou, M. Xu, Y. Zhou, H. Zhang, J. Han, F. Li and C. Huang, *Angew. Chem., Int. Ed.*, 2008, **47**, 1063–1067; (*b*) J. Wu, T. Yi, Q. Xia, Y. Zhou, F. Liu, J. Dong, T. Shu, F. Li and C. Huang, *Chem.–Eur. J.*, 2009, **15**, 6234–6243; (*c*) J. Wu, T. Yi, Y. Zou, T. Shu, F. Liu, H. Yan, F. Li, Z. Chen, Z. Zhou and C. Huang, *J. Mater. Chem.*, 2009, **19**, 3971–3978; (*d*) Y. Zhou, T. Yi, T. Li, Z. Zhou, F. Li, W. Huang and C. Huang, *Chem. Mater.*, 2006, **18**, 2974–2981.

7 (*a*) P. Terech and R. G. Weiss, *Chem. Rev.*, 1997, **97**, 3133–3159; (*b*) P. Cordier, F. Tournilhac, C. Soulié-Ziakovic and L. Leibler, *Nature*, 2008, **451**, 977–980; (*c*) R. P. Sijbesma, F. H. Beijer, L. Brunsveld, B. J. B. Folmer, J. H. K. Hirschberg, R. F. M. Lange, J. K. L. Lowe and E. W. Meijer, *Science*, 1997, **278**, 1601–1604; (*d*) L. A. Estroff and A. D. Hamilton, *Chem. Rev.*, 2004, **104**, 1201–1218; (*e*) K. J. C. van Bommel, A. Friggeri and S. Shinkai, *Angew. Chem., Int. Ed.*, 2003, **42**, 980–999; (*f*) J. M. Lehn, *Chem. Soc. Rev.*, 2007, **36**, 151–160.

8 K. Hyun, S. H. Kim, K. H. Ahn and S. J. Lee, *J. Non-Newtonian Fluid Mech.*, 2002, **107**, 51–65.

9 K. Hyun, J. G. Nam, M. Wilhellm, K. H. Ahn and S. J. Lee, *Rheol. Acta*, 2006, **45**, 239–249.

10 D. Bardelang, F. Camerel, J. C. Margeson, D. M. Leek, M. Schmutz, M. B. Zaman, K. Yu, D. V. Soldatov, R. Ziessel, C. I. Ratcliffe and J. A. Ripmeester, *J. Am. Chem. Soc.*, 2008, **130**, 3313–3315.

11 (*a*) H. A. Lashuel, S. R. LaBrenz, L. Woo, L. C. Serpell and J. W. Kelly, *J. Am. Chem. Soc.*, 2000, **122**, 5262; (*b*) A. Aggeli, M. Bell, N. Boden, J. N. Keen, P. F. Knowels, T. C. B. McLeish, M. Pitkeathly and S. E. Radford, *Nature*, 1997, **386**, 259; (*c*) K. Isozaki, H. Takaya and T. Naota, *Angew. Chem., Int. Ed.*, 2007, **46**, 2855–2857.

12 (*a*) H. Kunieda, K. Nakamura and D. F. Evans, *J. Am. Chem. Soc.*, 1991, **113**, 1051–1052; (*b*) K. P. Howard and J. H. Prestegard, *J. Am. Chem. Soc.*, 1996, **118**, 3345–3353; (*c*) O. Ohtani, H. Kato, T. Yui and K. Takagi, *J. Am. Chem. Soc.*, 2003, **125**, 14465–14472.

 This journal is © The Royal Society of Chemistry 2010